

Brief Article

An NMR biochemical assay for oxidosqualene cyclase: evaluation of inhibitor activities on *Trypanosoma cruzi* and human enzymes

Osamu Tani, Yukie Akutsu, Shinji Ito, Takayuki Suzuki, Yukihiko Tateishi, Tomohiko Yamaguchi, Tatsuya Niimi, Ichiji Namatame, Yasunori Chiba, Hitoshi Sakashita, Tomomi Kubota, Tetsuo Yanagi, Shusaku Mizukami, Kenji Hirayama, Koji Furukawa, and Kazuhiko Yamasaki

J. Med. Chem., **Just Accepted Manuscript** • DOI: 10.1021/acs.jmedchem.8b00484 • Publication Date (Web): 17 May 2018

Downloaded from <http://pubs.acs.org> on May 17, 2018

Just Accepted

“Just Accepted” manuscripts have been peer-reviewed and accepted for publication. They are posted online prior to technical editing, formatting for publication and author proofing. The American Chemical Society provides “Just Accepted” as a service to the research community to expedite the dissemination of scientific material as soon as possible after acceptance. “Just Accepted” manuscripts appear in full in PDF format accompanied by an HTML abstract. “Just Accepted” manuscripts have been fully peer reviewed, but should not be considered the official version of record. They are citable by the Digital Object Identifier (DOI®). “Just Accepted” is an optional service offered to authors. Therefore, the “Just Accepted” Web site may not include all articles that will be published in the journal. After a manuscript is technically edited and formatted, it will be removed from the “Just Accepted” Web site and published as an ASAP article. Note that technical editing may introduce minor changes to the manuscript text and/or graphics which could affect content, and all legal disclaimers and ethical guidelines that apply to the journal pertain. ACS cannot be held responsible for errors or consequences arising from the use of information contained in these “Just Accepted” manuscripts.



An NMR biochemical assay for oxidosqualene cyclase: evaluation of inhibitor activities on *Trypanosoma cruzi* and human enzymes

Osamu Tani¹, Yukie Akutsu¹, Shinji Ito², Takayuki Suzuki², Yukihiro Tateishi², Tomohiko Yamaguchi², Tatsuya Niimi², Ichiji Namatame², Yasunori Chiba³, Hitoshi Sakashita¹, Tomomi Kubota¹, Tetsuo Yanagi⁴,

Shusaku Mizukami⁴, Kenji Hirayama⁴, Koji Furukawa¹, and Kazuhiko Yamasaki^{1,*}

¹Biomedical Research Institute, National Institute of Advanced Industrial Science and Technology (AIST), 1-1-1 Higashi, Tsukuba, 305-8566, Japan.

²Drug Discovery Research, Astellas Pharma Inc., 21 Miyukigaoka, Tsukuba, 305-8585, Japan.

³Biotechnology Research Institute for Drug Discovery, National Institute of Advanced Industrial Science and Technology (AIST), 1-1-1 Umezono, Tsukuba, 305-8568, Japan.

⁴Department of Immunogenetics, Institute of Tropical Medicine, Nagasaki University, 1-12-4 Sakamoto, Nagasaki, 852-8523, Japan.

ABSTRACT: Oxidosqualene cyclase (OSC), a membrane-associated protein, is a key enzyme of sterol biosynthesis. Here we report a novel assay for OSC, involving reaction in aqueous solution, NMR quantification in organic solvent, and factor analysis of spectra. We evaluated one known and three novel inhibitors on OSC of *Trypanosoma cruzi*, a parasite causative of Chagas disease, and compared with their effects on human OSC for selectivity. Among them, one novel inhibitor showed a significant parasitocidal activity.

INTRODUCTION

Oxidosqualene cyclase (OSC; lanosterol synthase, E.C. 5.4.99.7) is a key enzyme in sterol biosynthesis, which catalyzes cyclization of 2,3-oxidosqualene to lanosterol with the multi-ring steroid scaffold^{1,2}. Successive enzymatic reactions lead to cholesterol in mammalian systems or ergosterol in fungal and protozoan systems. Because hypercholesterolemia is one of the major risks of arteriosclerosis, OSC inhibitors have been developed as candidate for nonstatin drugs to reduce cholesterol³⁻⁵. Also because disturbance of sterol biosynthesis impairs formation of membrane lipid bilayer, OSC is a highly potential target of developing antifungal drugs^{6,7}. For these purposes, a number of promising OSC inhibitors were designed and produced to date⁸. Indeed, established azole-type antifungal drugs, e.g., ketoconazole and posaconazole, inhibit lanosterol 14-demethylase (E.C. 1.14.13.70), a downstream enzyme of OSC^{9,10}. In addition, sterol $\Delta 8,7$ -isomerase (E.C. 5.3.3.5) and sterol $\Delta 14$ -reductase (E.C. 1.3.1.70) also in the downstream of OSC are targets of antifungal amorolfine¹¹.

Chagas disease is one of the worst neglected tropical diseases, with 10,000~14,000 people mostly in Latin America being deceased per year^{12,13}. This is caused by a protozoan parasite *Trypanosoma cruzi*, as transmitted by blood-sucking triatomine bugs. Two clinically used drugs, benznidazole and nifurtimox, are effective in acute phase, although they tend to be unsatisfactory in chronic phase, and have numerous toxic side effects^{12,13}.

Therefore, it is necessary to develop new drugs for Chagas disease. For this purpose, inhibitors were being investigated against a number of target proteins, such as a cysteine protease cruzain¹⁴, and a histone deacetylase sirtuin¹⁵.

Enzymes in sterol biosynthesis have been also chemotherapeutic targets against Chagas disease¹⁶. The antifungal azole-type inhibitors ketoconazole and posaconazole, inhibiting lanosterol 14-demethylase, and azasterol inhibitors against sterol $\Delta 24$ -methyltransferase (E.C. 2.1.1.43), have been shown to affect growth of *T. cruzi*¹⁷⁻¹⁹. Similarly, effects of numerous OSC inhibitors, including those originally developed for human OSC, were tested for *T. cruzi* OSC, and IC₅₀ values of nanomolar–micromolar level were obtained²⁰⁻²³. In animal, however, lanosterol depletion as a result of inhibition or mutational defect of OSC is known to cause lesions such as cataract^{24,25}. The importance of lanosterol in the lens was clearly demonstrated, in which treatment of the cataract-affected lens by lanosterol, but not by cholesterol, dissolved crystallin aggregation²⁶. Therefore, a usable inhibitor of *T. cruzi* OSC as a drug for Chagas disease should not affect the activity of human OSC, although it is not achieved at this moment²⁷.

To discover *T. cruzi* OSC-specific inhibitors, we need to evaluate a number of candidate compounds and, therefore, should employ an efficient method to measure enzymatic activity; it should be rapid and accurate as well. Nonetheless, the generally used assays for OSC are based on chromatography and radioactivity measurements^{1,2,4,20,21,23,28}, which appear to be time-

consuming and also are at a risk of radiation exposure. Namely, they utilize radioisotope-labeled substrates or precursors for the reaction. Then, typically after saponification of other types of lipids and extraction by hexane and/or ether, lanosterol was isolated by thin layer chromatography (TLC) for quantification. Alternatively, whole-cell assay using gas chromatography-mass spectrometry (GC-MS) to evaluate inhibitors of the sterol biosynthesis was reported^{29, 30}. This method is especially potential in identifying the target enzymes of inhibitors, although culture of cells takes one day to one week. Nonetheless, GC can be used for evaluating activity of recombinant OSC³¹.

In the process of exploration of novel inhibitors against another *T. cruzi* enzyme, we developed a novel method of biochemical assay by ¹H NMR measurement and factor analysis (FA)³² of the spectral data³³. The merits of ¹H NMR are that we can use non-labeled intact molecules for detection, and that we can deal with mixed sample, where individual molecules can be separately detected as spread peaks over the spectral region. Also, the merits of the FA treatment are that we can deal with all the data points in the spectral region of interest simultaneously, which is suitable for an automatic process, and that we can isolate meaningful change from baseline instability and/or noise and, thereby, obtain more accurate parameters for reaction and inhibition^{33, 34}.

In the present study, we developed an efficient biochemical assay for OSC, based on the previous NMR/FA method^{33, 34}. In the experimental protocol, a detergent as well as organic solvents were used, because OSC, a membrane-associated microsomal protein³⁵, and its substrate/product are insoluble to simple aqueous buffers. Inhibitory activities of one known and three new compounds against *T. cruzi* and human OSCs were evaluated and compared for the selectivity. In addition, we present a novel high-throughput method, which simultaneously processes data for different compounds by FA. These methods, in combination, are useful in many stages of drug discovery, e.g., from an initial screening stage of fragment-based drug discovery (FBDD)³⁶ to a final optimization stage.

RESULTS AND DISCUSSION

NMR biochemical assay of OSC. In the assay system for OSC, we must deal with water-insoluble substrate and product, 2,3-oxidosqualene and lanosterol, respectively. These materials were dissolved in the reaction buffer by detergent Triton X-100, which was also necessary to dissolve the membrane-associated and partly hydrophobic OSC protein. This detergent, however, disturbed NMR detection, probably because of interaction between the molecules and the large-molecular micelle of Triton X-100 (data not shown). Addition of organic solvent, therefore, was necessary to solubilize the molecules freely and to enable the NMR detection. We thus carried out a protocol shown in Fig. 1A. Namely, reaction proceeds at 37 °C in the aqueous solution containing detergent, and 10:1 methanol-D₂O mixture was added to stop the reaction and at the same time dissolve the substrate and product. Then, NMR measurements were carried out to detect substrate and/or product. Note that one may use deuterated methanol to simplify the spectrum, although the sharp methyl peak of methanol can be effectively reduced by a presaturation pulse (see Experimental section).

Although most of the NMR peaks originating from the substrate and product fully or partially overlap with many other peaks including those of detergent, two singlet peaks due to methyl groups of lanosterol³⁷ (19-H and 28-H; see Fig. S1 in the Supporting Information) were observed separately and used for

quantitative analyses (Fig. 2A). In order to evaluate enzymatic activity, reaction times were varied within 10–80 min and time-dependent changes of the NMR spectra were analyzed. To deal with the entire data points in a selected spectral region, FA was used as described previously (see also the Experimental section)^{33, 34}. By this treatment, loading vectors and score vectors are obtained for the respective “factors”, where the former represent spectral profile and the latter represent the time dependence in this case. The loading vector of the first factor that corresponds to the largest eigenvalue, but not those of the others, exhibited a profile reproducing the NMR peaks of lanosterol (Fig. 2B). Also, the score vector only of this factor showed a time-dependent change fitting an exponential curve (Fig. 2C). The first factor, therefore, clearly represents the time-dependent change of the population of lanosterol, that is, the enzymatic reaction of OSC. The kinetic constant for this reaction was calculated to be 0.083 min⁻¹ for *T. cruzi* OSC. By the same approach, a kinetic constant of 0.017 min⁻¹ was obtained for human OSC (Fig. S2). Note that the rates depend on the concentrations of enzymes, which should be set low enough to allow evaluation of strong inhibitors.

Evaluation of inhibitors. In the present study, one known inhibitor Ro 48-8071⁴ (compound **1** in Fig. 3) and three novel compounds (compounds **2–4** in Fig. 3) were tested for *T. cruzi* and human OSCs. In order to evaluate the inhibitory effects, a protocol shown in Fig. 1B was carried out, which involves a series of reactions with variable concentrations of the inhibitors at a constant time. Similarly to the above process for the time-dependent data, FA was applied to these concentration-dependent data (Fig. 4, Fig. S3). By fitting the score vector of the first factor with equations 3 and 4 in the methods section, the inhibitor concentration causing 50% inhibition (IC₅₀) was calculated. Compound **1** inhibited *T. cruzi* and human OSCs with IC₅₀ values of 13 and 7.5 nM, respectively (Table 1). It is noteworthy that this inhibitor is more effective to the human enzyme than to the *T. cruzi* enzyme. This selectivity is consistent with a previous study using the two enzymes expressed in *Saccharomyces cerevisiae*²³. Namely, the IC₅₀ values for *T. cruzi* and human OSCs were 0.90 and 0.17 μM, respectively.

By the same method, three novel compounds (**2–4**) were evaluated and IC₅₀ values were obtained (Table 1). The compound **2**, which has an allylmethylamine moiety similar to **1** (Fig. 3) showed 3-fold weaker inhibitory activity against *T. cruzi* OSC than **1** with an IC₅₀ value of 42 nM, and the selectivity against human OSC remained unchanged. Compound **3** showed inhibitory activity to *T. cruzi* OSC with an IC₅₀ value of 44 nM, which was comparable to that of **2**. However, compound **3** inhibited human OSC with an IC₅₀ value of 120 nM, that is, **3** is 2.7-fold more selective to *T. cruzi* OSC than human. Also, compound **4**, which is a dimethylamine analogue of **2**, showed inhibitory activity against *T. cruzi* and human OSC with IC₅₀ values of 140 and 230 nM, respectively. Considering that **3** and **4** showed selectivity to *T. cruzi* OSC, but allylmethylamines **1** and **2** did not, the dimethylamine moiety may contribute to the selectivity. While we understand that 3-fold selectivity is not large and distant from the goal, it can be a clue to acquire highly *T. cruzi* OSC-selective inhibitors. We should point out that a compound with a similar structure but lacking the dimethylamine moiety of **3** or **4** (compound 29 in ref. 38) was only effective to human OSC, but not to *T. cruzi* OSC.

Because **2** and **3** have stronger activity than **4**, we tested their effects on the proliferation of *T. cruzi* (Table 1). They indeed affected proliferation of the parasite in the epimastigote, corre-

sponding to the insect-hosted stage, by IC_{50} values of 110 and 2150 μM for **2** and **3**, respectively. Note that the effects are weaker than those against *T. cruzi* OSC, especially for **3**. This is probably because compounds should permeate through the cell membrane to reach OSC, which is a microsomal enzyme located inside the cell.

We further accessed the parasitocidal effects on the amastigote, corresponding to the intercellular stage, by duration until appearance of trypomastigote, a form generally seen in blood, after treatment of compounds (Table 2). Similarly to the above, **2** is stronger than **3**, with a longer duration of silence. It should be especially noted that **2** is significantly more effective than clinically used benznidazole.

A method suitable for initial screening. In drug discovery, throughput in an NMR analysis is frequently a matter to be discussed. Indeed the process of obtaining an IC_{50} value shown in Fig. 4 involves 12 sets of NMR measurements (a point relevant for absence of the inhibitor is not shown in Fig 4C). This requires approximately two hours including setup for the measurement, even if we use automatic measurement protocol, and is not suitable for the initial screening stage of FBDD starting from the fragment library.

To accelerate the drug discovery, we present here a simple protocol to evaluate multiple compounds simultaneously (Fig. 1C), in which inhibitor concentration as well as reaction time was fixed. Fig. 5 shows an application to the four inhibitory compounds on *T. cruzi* OSC. The NMR data were also processed by FA, with the score vectors corresponding to different compounds (Fig. 5). It should be noted that the score vector is nearly proportional to IC_{50} , having a correlation coefficient of 0.89. Therefore, this approach is useful in screening the compound library, in order to pick up candidates of inhibitory compounds. Once a compound is identified as a candidate of an inhibitor, the IC_{50} value should be determined for more accurate evaluation by the protocol shown in Fig. 1B. Application to human OSC is also shown in Fig. S4. Also, correlation between score vector and IC_{50} value was confirmed with a correlation coefficient of 0.94.

Assuming that approximately 10 min is required for the NMR measurements to evaluate a single compound, the initial screening of a fragment library of 1,000 compounds will take one week. When the rate of positive hit is low, we may use a mixed sample. Thus, when we use mixtures of e.g., 10 compounds each, the time required for the initial screening becomes within a single day.

Advantage of NMR biochemical assay for OSC. Optical detection systems including fluorescent system are most suitable for biochemical assay in drug discovery in terms of throughput, although they are not applicable to OSC currently. In such a situation, ^1H NMR detection is a powerful alternative, which is sensitive to almost all chemical conversions.

One of the merits of the present NMR method is that we do not need a radioactive substrate, in contrast to the conventional assays^{1, 2, 4, 20, 21, 23, 28}. Therefore, experiments can be carried out without care for exposure to radiation. Also, in an NMR spectrum, protons of different molecules exhibit peaks in different positions, although some of them overlap with each other. As far as we identify separate peaks originating from the molecule of interest, we can deal with samples mixed with other molecules, such as detergent. Therefore, we do not need chromatographic separation or saponification also in contrast with the conventional assays^{1, 2, 4, 20, 21, 23, 28} or GC(-MS) assays²⁹⁻³¹.

Especially by automatic measurements and FA data processing, the NMR assay for OSC is simple and with a considerable throughput. Because NMR is most useful in evaluating biophysical interaction between protein and compounds^{39, 40}, we may carry out biophysical binding assay by NMR, as well under a comparable condition. Thus, utilizing NMR for screening at different criteria will reduce pseudo-positive or pseudo-negative hits, and thereby improves the reliability of drug discovery processes.

EXPERIMENTAL SECTION

Sample preparation. The DNAs that code for oxidosqualene cyclase (E.C. number 5.4.99.7) of *Homo sapiens* and *T. cruzi* strain CL Brener (NCBI codes AAB36220 and XP_820967.1, respectively) were chemically synthesized (Thermo Fisher Scientific Inc., Waltham, MA) with the codon usage optimized for *Pichia pastoris*. After PCR amplification, the DNAs were subcloned into expression vector pPICZ B (Thermo Fisher Scientific), with myc-epitope and His₆ tag attached at the C-terminus. The *P. pastoris* cells (strain GS115) were grown in BMGY medium [1% yeast extract, 2% peptone, 100 mM potassium phosphate (pH 6.0), 1.34% yeast nitrogen base, 0.4 mg/L biotin, 0.5% glucose, 0.2% glycerol] at 30 °C for 3 days. Then, the proteins were expressed in BMMY medium [1% yeast extract, 2% peptone, 100 mM potassium phosphate (pH 6.0), 1.34% yeast nitrogen base, 0.4 mg/L biotin, 1% methanol] at 25 °C for 2 days.

After cells were lysed by high-pressure homogenizer Emulsi-Flex C5 (Avestin, Ottawa, Canada) in a buffer [50 mM Tris-HCl (pH 7.5), 250 mM NaCl, 5 μM pepstatin A (Sigma-Aldrich), 1 mM PMSF], and 0.5–1% Triton X-100 (Wako, Osaka, Japan) was added to the crude extract. Proteins were purified by column chromatography using HisTrap HP (GE Healthcare), and Resource Q (GE Healthcare) for *T. cruzi* OSC, and Superdex 200 (GE Healthcare), in addition to the above, for human OSC. Buffers used are: [20–50 mM Tris-HCl (pH 7.5–8.0), 5% glycerol, 0–250 mM imidazole, 0–500 mM NaCl, and 0.2% Triton X-100 or 0.2–1.2% β -octylglucoside (Nacalai, Kyoto, Japan)] for *T. cruzi* OSC and [20–50 mM Tris-HCl (pH 7.5–8.0), 5% glycerol, 0–250 mM imidazole, 0–500 mM NaCl, and 0.2% Triton X-100 or 0.2–0.8% β -octylglucoside (Nacalai)] for human OSC. The protein concentrations were determined by Pierce 660 nm protein assay reagent (Thermo Fisher Scientific.).

NMR assay for enzymatic activity. The brief protocol was illustrated as flow chart in Fig. 1A. The substrate 2,3-oxidosqualene (Sigma-Aldrich) was dissolved at the concentration of 100 μM in the reaction buffer [10 mM sodium phosphate (pH 7.0), 0.1% Triton X-100, 100 μM sodium 2,2-dimethyl-2-silapentane-5-sulfonate (DSS; Sigma-Aldrich), and 5% dimethylsulfoxide-d₆ (DMSO-d₆; Cambridge Isotope Laboratories Inc., Andover, MA)]. Reactions were initiated by adding enzyme to a final concentration of 19 nM, which were kept at 37 °C in a thermal cycler (Biometra, Göttingen, Germany) for 10–80 min, and stopped by adding 5-fold larger volumes of 10:1 mixture of methanol and 99% D₂O (Shoko, Tokyo, Japan). Samples were set in the cartridge of 96 tubes for a SampleJet automatic sample changer (Bruker BioSpin, Rheinstetten, Germany). ^1H NMR measurements of reaction solutions were carried out on an Avance III 500 spectrometer (Bruker BioSpin; 500.13 MHz) at 25 °C, automatically by ICON-NMR program module, where water and methanol signals were suppressed by

3-9-19 pulse sequence with the field gradient⁴¹ and presaturation, respectively.

The region of the spectra including the peaks of lanosterol was processed by means of FA³², as described previously³³. Briefly, a series of spectral data obtained with different reaction times were composed as data matrix **D**, with rows representing the chemical shifts and columns representing the reaction times. In **D**, the intensity was mean-centered along with the time axis and data points with change in the intensity less than twice the root-mean-square (rms) noise were excluded. Eigensystem analysis of covariance matrix

$$\mathbf{Z} = \mathbf{D}^T \mathbf{D} \quad (1)$$

where \mathbf{D}^T is the transposed matrix of **D**, was carried out in order to decompose **D** as

$$\mathbf{D} = \mathbf{R} \mathbf{C} + \mathbf{E} \quad (2)$$

In equation 2, **R** is the row matrix, with rows representing the chemical shifts and columns representing the factors, **C** is the column matrix with row representing the factors and column representing the reaction times, and **E** is the minimized error matrix. Note that matrix **C** is composed of its row vectors that are identical with the eigenvectors of **Z**. The column vectors of **R** show spectral profile for the factors, here called loading vectors, while the row vectors of **C** show time dependence of the factors, here called score vectors. In Figs 2–4, the score vectors, which are originally unit vectors, are multiplied by root of the respective eigenvalues, in order to express the degree of contribution. In order to obtain the kinetic constants of the reaction, the score vector of the first factor, with the largest eigenvalue, was fitted to an exponential curve.

Inhibitors. Compounds 1–4 were derived from the Astellas' chemical compound library. The synthetic routes were described in Supporting Information. The purities of the compounds were evaluated by ultra-high performance liquid chromatography to be higher than 95%, also as described in Supporting Information.

NMR assay for inhibitor activity. The flow chart for the inhibitor assay was shown in Fig. 1B. The solutions as described above except for supplement of various concentrations of inhibitors (0–100 μM) were placed in the wells of a 96-well plate designed for PCR. Reactions were initiated by adding 19 nM of enzyme at 37 °C, kept in a thermal cycler (Biometra) for 20 min for *T. cruzi* OSC or 90 min for human OSC, and stopped by adding 5-fold larger volumes of 10:1 mixture of methanol and 99% D₂O (Shoko). 1D ¹H NMR measurements were carried out at 25 °C as above.

The spectra obtained at different inhibitor concentrations were composed as data matrix **D** and FA calculation was carried out as described above. To estimate IC₅₀, the score vector with the largest eigenvalue was fitted simultaneously with

$$Y = A e^{-Vt} + B \quad (3)$$

and

$$V = \frac{V_0}{1 + [I]/IC_{50}} \quad (4)$$

where Y is the intensity in the score vector; *V* is the rate at different inhibitor concentrations; *t* is the fixed reaction time; A and B are variables for fitting, together with IC₅₀; *V*₀ is the rate without inhibitor, which was determined in advance, as described above; and [*I*] is the concentration of inhibitor. Note that equation 4 is deduced from Cheng and Prusoff⁴². The error level for IC₅₀ was estimated by a Monte Carlo simulation that randomizes the data as Gaussian distributions with the standard deviation of the initial fitting residuals.

For simultaneous evaluation of inhibitory activities of a series of compounds (Fig. 1C), the spectra obtained for different inhibitor compounds were composed as data matrix **D** and FA calculation was carried, as above.

Antiproliferation and parasiticidal activities. For evaluation of antiproliferation effects, one million of epimastigote culture form of *T. cruzi*, Tulahuen strain, obtained through NEKKEN Bio-resource Center (Nagasaki, Japan) in LIT culture medium supplemented with 10% newborn calf serum were co-incubated with the test compound. After culture, alamarBlue test solution (Thermo Scientific) was added to the media, for which fluorescence intensity was monitored to evaluate the viability.

For evaluation of parasiticidal activity, purified trypomastigote parasites were applied to a 24-well plate confluent covered by the NIH 3T3 fibroblast, and incubated for two days. Then the residual floating trypomastigotes were washed out. After culture for 5 days, the test compound was added and incubated for 5 days, and for another 10 days with a fresh compound. After washing out the compound, the duration until a new trypomastigote emerged from the infected cells was observed. As a positive control, benznidazole was used.

ASSOCIATED CONTENT

Supporting Information

The Supporting Information is available free of charge on the ACS Publications website at DOI:

Methods for chemical syntheses and supplementary figures illustrating chemical structure and an NMR spectrum of lanosterol (Fig. S1) and NMR analyses on human OSC (Figs. S2-4) (PDF)

Molecular Formula Strings (CSV)

AUTHOR INFORMATION

Corresponding Author

* Phone: +81-29-8619473. Fax: +81-29-8612706. E-mail: k-yamasaki@aist.go.jp

Author Contributions

The manuscript was written through contributions of all authors.

Notes

The authors declare no competing interest.

ACKNOWLEDGMENT

This project was supported by Leading Engine program for Accelerating Drug discovery (LEAD) of AIST. We thank members of the Consortium for Neglected Tropical Diseases participating from Astellas Pharma Inc., Drugs for Neglected Diseases initiative (DNDi), Tokyo Institute of Technology, High Energy Accelerator Research Organization, AIST, Nagasaki University, and University of Tokyo for helpful discussions and advice.

ABBREVIATIONS USED

DMSO, dimethylsulfoxide; FA, factor analysis; DSS, sodium 2,2-dimethyl-2-silapentane-5-sulfonate; FBDD, fragment-based drug discovery; GC-MS, gas chromatography-mass spectrometry; IC₅₀, the inhibitor concentration causing 50% inhibition; OSC, ox-

idosqualene cyclase; rms, root mean square; TLC, thin layer chromatography

REFERENCES

- (1) Corey, E. J.; Russey, W. E.; Ortiz de Montellano, P. R. 2,3-Oxidosqualene an intermediate in biological synthesis of sterols from squalene. *J. Am. Chem. Soc.* **1966**, *88*, 4750-4751.
- (2) Van Tamelen, E. E.; Willett, J. D.; Clayton, R. B.; Lord, K. E. Enzymic conversion of squalene 2,3-oxide to lanosterol and cholesterol. *J. Am. Chem. Soc.* **1966**, *88*, 4752-4754.
- (3) Mark, M.; Muller, P.; Maier, R.; Eisele, B. Effects of a novel 2,3-oxidosqualene cyclase inhibitor on the regulation of cholesterol biosynthesis in HepG2 cells. *J. Lipid Res.* **1996**, *37*, 148-158.
- (4) Morand, O. H.; Aebi, J. D.; Dehmlow, H.; Ji, Y. H.; Gains, N.; Lengsfeld, H.; Himber, J. Ro 48-8071, a new 2,3-oxidosqualene:lanosterol cyclase inhibitor lowering plasma cholesterol in hamsters, squirrel monkeys, and minipigs: comparison to simvastatin. *J. Lipid Res.* **1997**, *38*, 373-390.
- (5) Dehmlow, H.; Aebi, J. D.; Jolidon, S.; Ji, Y. H.; von der Mark, E. M.; Himber, J.; Morand, O. H. Synthesis and structure-activity studies of novel orally active non-terpenoid 2,3-oxidosqualene cyclase inhibitors. *J. Med. Chem.* **2003**, *46*, 3354-3370.
- (6) Cattell, L.; Ceruti, M.; Viola, F.; Delprino, L.; Balliano, G.; Duriatti, A.; Bouvier-Nave, P. The squalene-2,3-epoxide cyclase as a model for the development of new drugs. *Lipids* **1986**, *21*, 31-38.
- (7) Jolidon, S.; Polak, A. M.; Guerry, P.; Hartman, P. G. Inhibitors of 2,3-oxidosqualene lanosterol-cyclase as potential antifungal agents. *Biochem. Soc. Trans.* **1990**, *18*, 47-48.
- (8) Rabelo, V. W.; Romeiro, N. C.; Abreu, P. A. Design strategies of oxidosqualene cyclase inhibitors: targeting the sterol biosynthetic pathway. *J. Steroid Biochem. Mol. Biol.* **2017**, *171*, 305-317.
- (9) Miettinen, T. A. Cholesterol metabolism during ketoconazole treatment in man. *J. Lipid Res.* **1988**, *29*, 43-51.
- (10) Ghannoum, M. A.; Rice, L. B. Antifungal agents: mode of action, mechanisms of resistance, and correlation of these mechanisms with bacterial resistance. *Clin. Microbiol. Rev.* **1999**, *12*, 501-517.
- (11) Polak, A. M. Preclinical data and mode of action of amorolfine. *Clin. Exp. Dermatol.* **1992**, *17 Suppl 1*, 8-12.
- (12) World Health Organization. Research priorities for Chagas disease, human African trypanosomiasis and leishmaniasis. *W. H. O. Tech. Rep. Ser.* **2012**, 975, i-xii, 1-100, WHO Press, Geneva, Switzerland.
- (13) Rogers, N. Bugging out over Chagas: Bioluminescent protozoans and old drugs might help unravel kissing-bug disease. *Nat. Med.* **2015**, *21*, 1108-1110.
- (14) Engel, J. C.; Doyle, P. S.; Hsieh, I.; McKerrow, J. H. Cysteine protease inhibitors cure an experimental *Trypanosoma cruzi* infection. *J. Exp. Med.* **1998**, *188*, 725-734.
- (15) Veiga-Santos, P.; Reignault, L. C.; Huber, K.; Bracher, F.; De Souza, W.; De Carvalho, T. M. Inhibition of NAD⁺-dependent histone deacetylases (sirtuins) causes growth arrest and activates both apoptosis and autophagy in the pathogenic protozoan *Trypanosoma cruzi*. *Parasitology* **2014**, *141*, 814-825.
- (16) Urbina, J. A. Lipid biosynthesis pathways as chemotherapeutic targets in kinetoplastid parasites. *Parasitology* **1997**, *114 Suppl*, S91-99.
- (17) Beach, D. H.; Goad, L. J.; Holz, G. G., Jr. Effects of ketoconazole on sterol biosynthesis by *Trypanosoma cruzi* epimastigotes. *Biochem. Biophys. Res. Commun.* **1986**, *136*, 851-856.
- (18) Urbina, J. A.; Vivas, J.; Visbal, G.; Contreras, L. M. Modification of the sterol composition of *Trypanosoma (Schizotrypanum) cruzi* epimastigotes by delta 24(25)-sterol methyl transferase inhibitors and their combinations with ketoconazole. *Mol. Biochem. Parasitol.* **1995**, *73*, 199-210.
- (19) Urbina, J. A.; Payares, G.; Contreras, L. M.; Liendo, A.; Sanoja, C.; Molina, J.; Piras, M.; Piras, R.; Perez, N.; Wincker, P.; Loebenberg, D. Antiproliferative effects and mechanism of action of SCH 56592 against *Trypanosoma (Schizotrypanum) cruzi*: in vitro and in vivo studies. *Antimicrob. Agents Chemother.* **1998**, *42*, 1771-1777.
- (20) Buckner, F. S.; Griffin, J. H.; Wilson, A. J.; Van Voorhis, W. C. Potent anti-*Trypanosoma cruzi* activities of oxidosqualene cyclase inhibitors. *Antimicrob. Agents Chemother.* **2001**, *45*, 1210-1215.
- (21) Oliaro-Bosso, S.; Ceruti, M.; Balliano, G.; Milla, P.; Rocco, F.; Viola, F. Analogs of squalene and oxidosqualene inhibit oxidosqualene cyclase of *Trypanosoma cruzi* expressed in *Saccharomyces cerevisiae*. *Lipids* **2005**, *40*, 1257-1262.
- (22) Benaim, G.; Sanders, J. M.; Garcia-Marchan, Y.; Colina, C.; Lira, R.; Caldera, A. R.; Payares, G.; Sanoja, C.; Burgos, J. M.; Leon-Rossell, A.; Concepcion, J. L.; Schijman, A. G.; Levin, M.; Oldfield, E.; Urbina, J. A. Amiodarone has intrinsic anti-*Trypanosoma cruzi* activity and acts synergistically with posaconazole. *J. Med. Chem.* **2006**, *49*, 892-899.
- (23) Balliano, G.; Dehmlow, H.; Oliaro-Bosso, S.; Scaldaferrri, M.; Taramino, S.; Viola, F.; Caron, G.; Aebi, J.; Ackermann, J. Oxidosqualene cyclase from *Saccharomyces cerevisiae*, *Trypanosoma cruzi*, *Pneumocystis carinii* and *Arabidopsis thaliana* expressed in yeast: a model for the development of novel antiparasitic agents. *Bioorg. Med. Chem. Lett.* **2009**, *19*, 718-723.
- (24) Pyrah, I. T.; Kalinowski, A.; Jackson, D.; Davies, W.; Davis, S.; Aldridge, A.; Greaves, P. Toxicologic lesions associated with two related inhibitors of oxidosqualene cyclase in the dog and mouse. *Toxicol. Pathol.* **2001**, *29*, 174-179.
- (25) Mori, M.; Li, G.; Abe, I.; Nakayama, J.; Guo, Z.; Sawashita, J.; Ugawa, T.; Nishizono, S.; Serikawa, T.; Higuchi, K.; Shumiya, S. Lanosterol synthase mutations cause cholesterol deficiency-associated cataracts in the Shumiya cataract rat. *J. Clin. Invest.* **2006**, *116*, 395-404.
- (26) Zhao, L.; Chen, X. J.; Zhu, J.; Xi, Y. B.; Yang, X.; Hu, L. D.; Ouyang, H.; Patel, S. H.; Jin, X.; Lin, D.; Wu, F.; Flagg, K.; Cai, H.; Li, G.; Cao, G.; Lin, Y.; Chen, D.; Wen, C.; Chung, C.; Wang, Y.; Qiu, A.; Yeh, E.; Wang, W.; Hu, X.; Grob, S.; Abagyan, R.; Su, Z.; Tjondro, H. C.; Zhao, X. J.; Luo, H.; Hou, R.; Perry, J. J.; Gao, W.; Kozak, I.; Granet, D.; Li, Y.; Sun, X.; Wang, J.; Zhang, L.; Liu, Y.; Yan, Y. B.; Zhang, K. Lanosterol reverses protein aggregation in cataracts. *Nature* **2015**, *523*, 607-611.
- (27) Fouchet, M. H.; Donche, F.; Martin, C.; Bouillot, A.; Junot, C.; Boullay, A. B.; Potvain, F.; Magny, S. D.; Coste, H.; Walker, M.; Issandou, M.; Dodic, N. Design and evaluation of a novel series of 2,3-oxidosqualene cyclase inhibitors with low systemic exposure, relationship between pharmacokinetic properties and ocular toxicity. *Bioorg. Med. Chem.* **2008**, *16*, 6218-6232.
- (28) Lenhart, A.; Reinert, D. J.; Aebi, J. D.; Dehmlow, H.; Morand, O. H.; Schulz, G. E. Binding structures and potencies of oxidosqualene cyclase inhibitors with the homologous squalene-hopene cyclase. *J. Med. Chem.* **2003**, *46*, 2083-2092.
- (29) Giera, M.; Plossl, F.; Bracher, F. Fast and easy in vitro screening assay for cholesterol biosynthesis inhibitors in the post-squalene pathway. *Steroids* **2007**, *72*, 633-642.
- (30) Müller, C.; Binder, U.; Bracher, F.; Giera, M. Antifungal drug testing by combining minimal inhibitory concentration testing with target identification by gas chromatography-mass spectrometry. *Nat. Protoc.* **2017**, *12*, 947-963.
- (31) Nakano, C.; Motegi, A.; Sato, T.; Onodera, M.; Hoshino, T. Sterol biosynthesis by a prokaryote: first in vitro identification of the genes encoding squalene epoxidase and lanosterol synthase from *Methylococcus capsulatus*. *Biosci. Biotechnol. Biochem.* **2007**, *71*, 2543-2550.
- (32) Malinowski, E. R. *Factor Analysis in Chemistry*. 3rd ed.; Wiley: New York, 2002.
- (33) Yamasaki, K.; Tani, O.; Tateishi, Y.; Tanabe, E.; Namatame, I.; Niimi, T.; Furukawa, K.; Sakashita, H. An NMR biochemical Assay for fragment-based drug discovery: evaluation of an inhibitor activity on spermidine synthase of *Trypanosoma cruzi*. *J. Med. Chem.* **2016**, *59*, 2261-2266.
- (34) Yamasaki, K.; Obara, Y.; Hasegawa, M.; Tanaka, H.; Yamasaki, T.; Wakuda, T.; Okada, M.; Kohzuma, T. Real-time NMR monitoring of protein-folding kinetics by a recycle flow system for temperature jump. *Anal. Chem.* **2013**, *85*, 9439-9443.
- (35) Yamamoto, S.; Lin, K.; Bloch, K. Some properties of the microsomal 2,3-oxidosqualene sterol cyclase. *Proc. Natl. Acad. Sci. U. S. A.* **1969**, *63*, 110-117.
- (36) Erlanson, D. A.; McDowell, R. S.; O'Brien, T. Fragment-based drug discovery. *J. Med. Chem.* **2004**, *47*, 3463-3482.
- (37) Emmons, G. T.; Wilson, W. K.; Schroepfer, G. J. ¹H and ¹³C NMR assignments for lanostan-3 β -ol derivatives: revised assignments for lanosterol. *Magn. Reson. Chem.* **1989**, *27*, 1012-1024.
- (38) Keller, M.; Wölgardt, A.; Müller, C.; Wilcken, R.; Bockler, F. M.; Oliaro-Bosso, S.; Ferrante, T.; Balliano, G.; Bracher, F. Arylpiperidines as a new class of oxidosqualene cyclase inhibitors. *Eur. J. Med. Chem.* **2016**, *109*, 13-22.
- (39) Dalvit, C. Efficient multiple-solvent suppression for the study of the interactions of organic solvents with biomolecules. *J. Biomol. NMR* **1998**, *11*, 437-444.
- (40) Mayer, M.; Meyer, B. Group epitope mapping by saturation transfer difference NMR to identify segments of a ligand in direct contact with a protein receptor. *J. Am. Chem. Soc.* **2001**, *123*, 6108-6117.

(41) Piotta, M.; Saudek, V.; Sklenar, V. Gradient-tailored excitation for single-quantum NMR spectroscopy of aqueous solutions. *J. Biomol. NMR* **1992**, *2*, 661-665.

(42) Cheng, Y.; Prusoff, W. H. Relationship between the inhibition constant (KI) and the concentration of inhibitor which causes 50 per cent inhibition (I50) of an enzymatic reaction. *Biochem. Pharmacol.* **1973**, *22*, 3099-3108.

Table 1: IC₅₀ values of inhibitor compounds against *T. cruzi* and human OSCs and proliferation of epimastigote (nM)

Compounds	Source of the enzyme		Ratio of IC ₅₀ (human/ <i>T. cruzi</i>)	Anti-proliferation
	<i>T. cruzi</i>	human		
1 (Ro 48-8071)	13±3	7.5±0.8	0.59	N. D. ^a
2	42±12	16±3	0.38	110
3	44±12	120±20	2.7	2150
4	140±50	230±40	1.6	N. D. ^a

^aNot determined.

Table 2: Parasitocidal activity evaluated by durations until detection of trypomastigote (days)

Compounds	Concentration of compounds	
	~10 μM ^a	~20 μM ^b
2	62±6	80±11
3	21±0	29±0.4
benznidazole	35±8	53±9

^a9.6, 10.9, and 9.6 μM for 2, 3, and benznidazole, respectively.

^bTwice the concentration of ~10 μM.

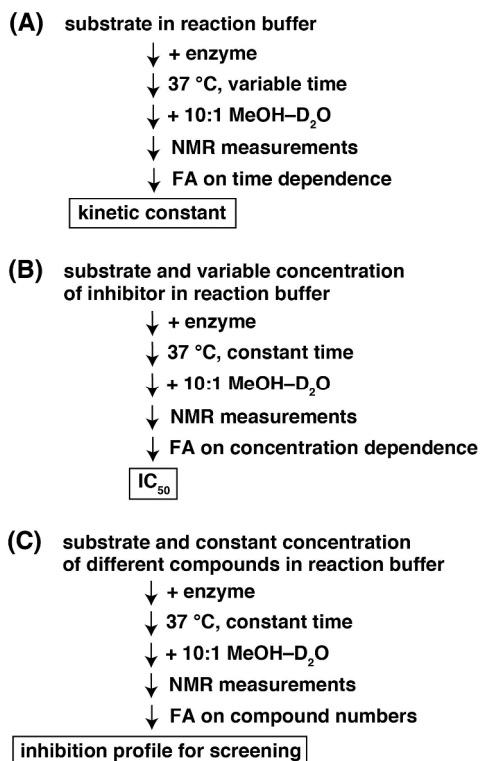


Figure 1. Protocols of the NMR biochemical assays for OSC: (A) evaluation of enzymatic activity, which yields kinetic constants, (B)

evaluation of inhibitors, which yields IC₅₀ values, and (C) simultaneous evaluation of inhibitory activities of a series of compounds, applicable to screening of the fragment library.

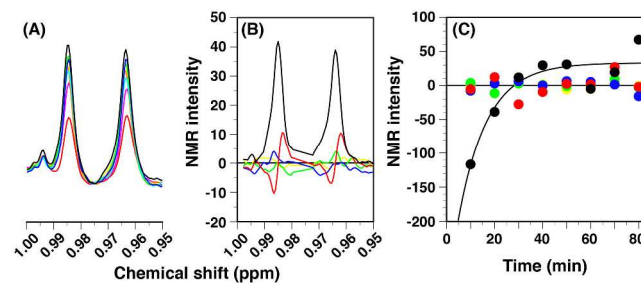


Figure 2. NMR analysis on the enzymatic activity of *T. cruzi* OSC. (A) NMR spectra of reactants after the protocol shown in Fig. 1A. A spectral region contains the NMR peaks originating from the product, lanosterol (28-H at 0.984 ppm and 19-H at 0.963 ppm). Reactions were conducted at 37 °C for 10 (red), 20 (orange), 30 (yellow), 40 (green), 50 (cyan), 60 (blue), 70 (black) min. (B) FA loading vectors, representing the spectral profile, with lengths equal to the root of respective eigenvalues. Those of factors relevant for the five largest eigenvalues are selected; the first (black), second (red), third (blue), fourth (green) and fifth (yellow) factors ordered by eigenvalue. NMR intensity was normalized to rms noise. (C) FA score vectors, which represent the time dependence, also with lengths equal to the root of respective eigenvalues. Coloring scheme is the same as in (B). Exponential curve fitting for that of the first factor yields a kinetic constant of 0.083 min⁻¹.

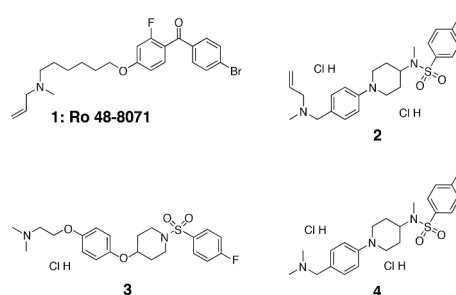


Figure 3. Inhibitor compounds evaluated in the present study. Compound numbers are the same as those in Table 1.

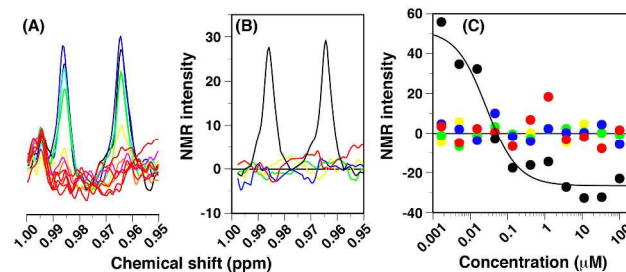
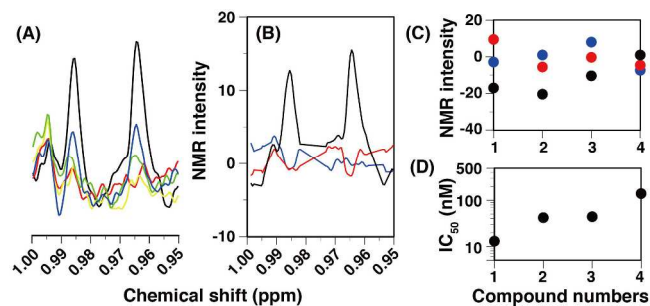


Figure 4. Inhibition of *T. cruzi* OSC by Ro 48-8071 (compound 1). (A) NMR spectra of reactants after the protocol shown in Fig. 1B. As in Fig. 2, the spectral region containing the NMR peaks of lanosterol was shown. Reactions were carried out at 37 °C for 20 min in the absence (black) or presence of different concentrations of compound 1, i.e., 0.0017 (blue), 0.051 (cyan), 0.015 (green), 0.046 (yellow), 0.14 (orange), 0.41 (magenta), and above 1.0 μM (1.2, 3.7, 11, 33, and 100 μM; red). (B) FA loading vectors representing the spectral profile. (C) FA score vectors representing the dependence on inhibitor concentrations. Curve fitting of that of the

1 first factor with equations 3 and 4 yields an IC_{50} value of 13 nM. In
2 (B) and (C), schemes for color and normalization of the intensities
3 were the same as those in Figure 2.



15 Figure 5. A high-throughput analysis on inhibition of *T. cruzi* OSC
16 by a series of compounds. (A) NMR spectra of reactants after the
17 protocol shown in Fig. 1C. Reactions were carried out at 37 °C for
18 20 min in the absence (black) or presence of either of 4 compounds
19 shown in Fig. 3 at 0.41 μ M (1: red; 2: yellow, 3: green, 4: blue). (B)
20 FA loading vectors representing spectral profile. (C) FA score vec-
21 tors indicating inhibition profile of compounds. The compound num-
22 bers are the same as those in Fig. 3 and Table 1. In (B) and (C),
23 schemes for color and normalization in intensity were the same as
24 those in Figs. 2 and 4, although the first three factors are shown
25 here. (D) IC_{50} values of the same compounds.

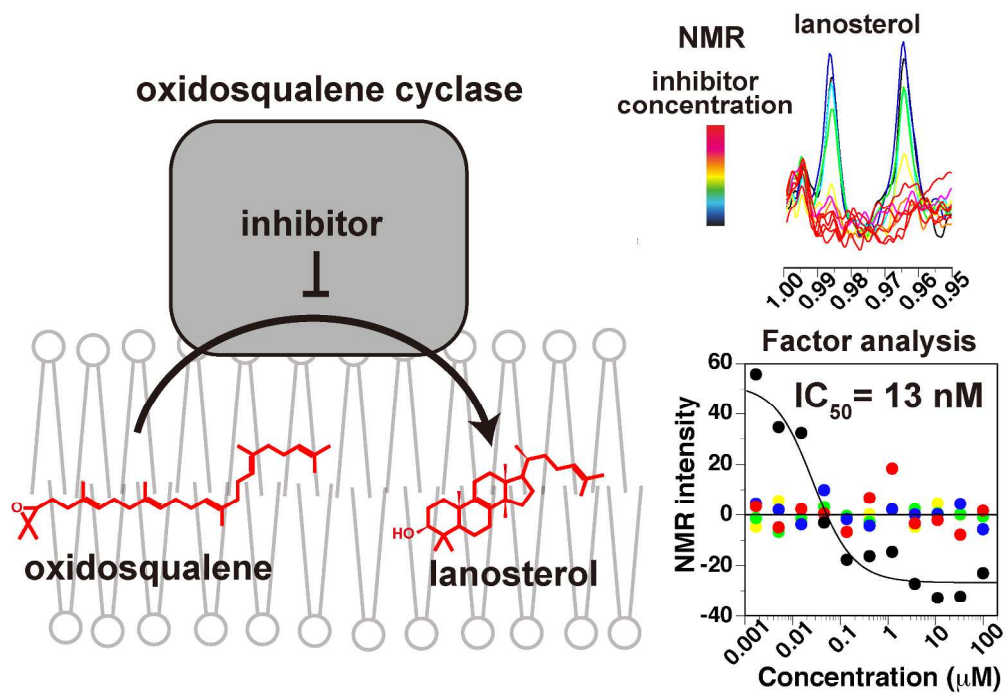


Table of content graphics

238x164mm (300 x 300 DPI)